714472

TERMINAL PROGRESS REPORT

PRECLINICAL STUDIES FOR PION RADIOTHERAPY

Grant No. 5-P01-CA-14052-06

Principal Investigator:

Morton M. Kligerman, M.D.
Director,
Cancer Research and Treatment Center
University of New Mexico
900 Camino de Salud
Albuquerque, New Mexico 87131

FILE BARCODE
00133339

COPIED FOR
HSPT

1091209

00133339.001

LANL

I. INTRODUCTION

A. Background

The grant award for Preclinical Studies for Pion Radiotherapy was originally made, effective 1 June 1973, to permit work to begin on the physics and biology associated with clinical pion radiotherapy. Clinical studies began on 1 May 1974 under a separate grant, CA-16127. The two grants ran in parallel under the direction of Morton M. Kligerman, M.D., until 1 May 1979, at which time support for the physics and biology work was incorporated in CA-16127. These projects have been conducted jointly by the University of New Mexico Cancer Research and Treatment Center and the Los Alamos Scientific Laboratory, using the pion biomedical channel of the Clinton P. Anderson Meson Physics Facility (LAMPF) in Los Alamos.

B. Period Covered by This Report

The combined grant application, submitted 1 June 1978, contains a summary report on the progress of the work in physics and biology under this grant up to 30 April 1978. This report updates that information to 30 April 1979, the terminal date of this grant.

II. PHYSICS

The total physics effort has been designed to obtain information and develop systems needed for clinical trials of pion radiotherapy.

Operation of the main proton accelerator at LAMPF was increased to 300 microamps on 31 August 1977; between June 1978 and April 1979, the accelerated proton current was increased from 360 to 500 microamps, 50% of the design goal. A water-cooled pion production target was developed and tested at proton currents up to 700 microamps. In the fall of 1979, production will be between 500 and 600 microamps.

A. Channel Operation and Control System Development

Major accomplishments include preparation of hardware and software systems for dynamic treatment, as well as improved reliability of hardware and software, including treatment couch systems; simulation systems; computerized channel control and operating systems; magnet control systems; dynamic collimating systems; dosimetry and microdosimetry data acquisition systems; and patient-monitoring and record-keeping systems. The new range-shifter control system was improved in control, maintenance, and noise suppression, and a new range-shifter was installed in the fall of 1978.

B. Channel Tuning/Beam Development

The catalog of broad beams for static treatments has been expanded to cover fields up to 17 cm x 17 cm at the 90 percent isodose line, 18 cm x 18 cm at the 80 percent isodose line, and 19.5 cm x 19.5 cm at the 50 percent isodose line. Fan beams for dynamic treatments have been prepared at several channel momenta with various sizes for the long dimension (X) of the beam perpendicular to the scan axis. The largest available size is 18 cm. Along

COPIED FOR
HSPT

1091210

00133339.002

LANL

the scan direction (Y) the beam is small (2.5 cm full width at half maximum) and highly focused. The field size in this dimension is controlled by the couch scan. The location of the (Y) beam waist (the Z value where the beam is the smallest) should be approximately in the center of the treatment volume. Fan tunes have been designed for two waist locations.

Improvements in time-of-flight identification of beam contamination have been made. Larger scintillators to handle the new large beams and the accelerator radio-frequency signal have been added. Combining the drift time between scintillators with the drift time from the target allows much improved separation of negative muons (μ^-) from negative pions (π^-). At present μ^-/π^- ratios of 0.2 are observed. The undetected muon fraction (from pion decay in the downstream part of the channel) is being calculated.

New water-cooled targets have allowed minimization and stabilization of electron contamination, as well as accurate proton beam steering and spot site measurements. These factors strongly influence pion beam position and momentum spread at the channel exit.

C. Dosimetry

The dosimetry effort has been directed mainly toward providing a large variety of patient beams and range-shifter functions and characterizing these for patient treatment. After the development of raw beams, the major effort has been to tailor the beams for individual treatment situations and to characterize these beams, incorporating into the dosimetry the effect of compensating bolus, collimators and the air gaps between patient treatment devices. Isodose distributions, in three dimensions, and the calibration of the dose rate and response of the pion monitor chambers are measured for each treatment configuration. Single-port measurements are then combined to obtain dosimetry for overlapping, opposed and adjacent or opposed, abutting ports.

All treatment beams derive from three basic beam penetrations: 12, 16, and 23 gm/cm^2. Using these three beams, any tumor between the skin surface and 23 gm/cm^2 in depth can be reached by using the appropriate bolus and range-shifting material. For each beam penetration, three beams have been developed which give different lateral dimensions. For all beams it is possible to spread the stopping region using the range-shifter. The range-shifter is programmed to give stopping pion distributions ranging in depth from 3 to 14 cm in 1 cm intervals.

For each spread peak it is possible to tailor the slope of the physical dose, and consequently the slope of distribution of stopping pions. Range-shifter functions have been developed to produce different slopes to study the effect of changes in total dose and stopping pion distribution on the RBE across the spread peak. When opposed, overlapping treatment fields are used, the resultant total dose and stopping pion distributions are relatively flat regardless of the slopes of the single port distributions. At the present time, using static beams, treatment of large fields (greater than 15 cm x 15 cm) is best accomplished by using abutting fields. While treatments with static pion fields give good distribution in two dimensions, a fan or spot beam delivered in scanning dynamic treatments will be needed to give variable transverse distribution in depth. The primary advantages of dynamic beam over static beam pion therapy are the dose uniformity along their scanning

COPIED FOR
HSPT
1091211
00133339.003
LANL

dimension(s) and the ability to better shape the pion beam so that normal tissue sparing is enhanced. Work is continuing for implementation of dynamic beam treatment.

Derivation of conversion factors for determining absorbed dose has produced preliminary values for incorporation into patient treatment planning. Measurements with tissue-equivalent and carbon calorimeters in the spring of 1979 confirmed that the preliminary conversion factors were within a few percent accuracy. Evaluation of whole-body dose indicates star-produced neutrons do not significantly reduce the dose localization properties of pions.

D. Microdosimetry

1. Ionization Chamber Microdosimetry

An alternative system for microdosimetric studies of therapeutic pion beams has been tested. This system utilizes a commercial (EG&G LET-½) detector that is 0.5 inches in diameter, but which has an effective diameter of 2 microns. The system is simple to use, but is limited to low count rates. Preliminary tests were made on low intensity proton beams (20-200 na protons). Spectra were taken for positive and negative pion beams with and without the range-shifter. A comparison of these data with previous results shows good agreement. Additional measurements were made at selected positions on three clinical pion beams to aid in the development of new range-shifter functions.

2. Silicon Detector Microdosimetry

Significant improvements have been made in the experimental data acquisition system, including noise reduction, installation of a pulse-pileup rejector and deadtime meter, improved gating system, and calibration and testing of thinner (5 and 7 μm thick) detectors. A series of Monte Carlo computer codes has been used in the interpretation of these experiments. The calculational effort is aimed at developing and testing various algorithms used in determining pion stopping distributions, absolute star dose, and LET distributions from the experimental data.

An intercomparison between microdosimetric spectra obtained with silicon detectors and a Rossi chamber has been completed. Various methods of comparison and data unfolding (to obtain both lineal energy spectra and LET spectra) were tested, and apparent differences between the two systems are now well understood. Monte Carlo generated spectra also agree well with the experimental results.

Measurements have been made and dose distributions have been evaluated for most of the therapeutic beams. A catalog has been prepared of high-LET dose distributions. Curves exist for unrange-shifted and range-shifted beam. The effect of collimators has also been studied. These data are now being used to recalculate all of the range-shifter functions used in therapy.

This method is also being used for *in vivo* measurements in patients, to check the treatment plan. A new *in vivo* technique has been

COPIED FOR
KSPT

00133339.004

1091212

LANL

developed which times the passage of the high-LET peak with respect to the position of the range-shifter. This measurement gives the average water equivalent of the tissues in front of the detector in a patient. This is a very useful check for treatment planning. In addition, the full width at half maximum of the observed high-LET distribution shows the effect of the inhomogeneities and gives a measure of their extent.

The high-LET scanning of a beam in a phantom is also being applied to a study of bolus discontinuities. The step discontinuity has been studied extensively and shows how the pion stopping distribution varies as one goes from one layer to a layer of increased thickness. A thorough study of the effect of different discontinuities is planned for the future.

E. In Vivo Dosimetry

Methods of in vivo dosimetry have been developed for use with pion radiotherapy patients. These dosimeters include TLD 700, aluminum activation, ionization chambers, and silicon detectors. Using combinations of these dosimeters, both the high-LET and total dose can be measured in vivo and these measurements are now done routinely on every patient for treatment verification

F. Visualization of Stopping Pion Distribution

Using high-energy gamma rays produced as a result of negative pion capture, a visualization experiment has demonstrated one-dimensional (Z) visualization with good spatial resolution using typical fractionated treatment doses and dose rates. Important backgrounds have been identified and eliminated. One patient treatment has been observed with the system. Future effort will include improving the present chamber or installing one designed for higher rates and performing more measurements on patients. Methods for using the data in routine treatment must then be determined.

Preliminary measurements with a positron detection system on patients with lesions of the pancreas, rectum, head and neck, and lung indicate that diffusion rates of activity from these sites should not be a limiting factor in measurements. Two NaI crystals have been purchased and will be used to test the feasibility of low-cost one-dimensional Anger camera for positron detection. Hardware tests for determination of detector configuration to provide for optimal resolution are underway. Also, software development for the data aquisition system is underway.

G. Beam Shaping

Measurements have been made for inhomogeneity and bolus compensation for pion beams of different energy; variation of the inhomogeneity depth beneath the surface; air and Teflon inhomogeneities to simulate lung and bone; bolus compensation using the parallel beam model; and bolus inhomogeneity misalignment. Compensation is the technique of modifying the pion beam so that the peak pion dose is constrained between the distal and proximal surfaces of the treatment volume. The penetration of the beam to the distal surface can be controlled either by using bolus to modify a monoenergetic beam or by varying the energy of a narrow beam as it scans the tumor volume. The proximal

COPIED FOR
HSPT

1091213

00133339.005

LANL

edge of the peak dose is controlled by properly modulating the pion peak width using a range-shifter. With static treatments, the proximal edge cannot be varied once the distal edge is defined. The implementation of dynamic scanning treatment will allow the proximal edge to vary as the treatment volume is scanned by varying the range-shifter function.

In designing the bolus, one must compensate for skin contour, tumor shape, tissue inhomogeneities, and patient motion. To utilize the information obtained from CT scans the patient must be scanned in a position which simulates as closely as possible the position in which the treatment is given. This is accomplished by making Lightcast forms of the patient. CT scans are usually taken at 1.0 cm intervals throughout the volume of interest which includes generous margins surrounding the tumor volume. The CT scan negative is then used to define the exact treatment volume. The tape containing CT scan data is read into the pion treatment-planning code, and the treatment volume marked on the CT scan negative is superimposed on a density image presented on a cathode ray tube. The treatment planner, using cursers, then locates the pion stopping region on the screen, inputting the appropriate pion range and range-shifter function. The computer code then calculates the thickness and shape of bolus (paraffin) required to stop the pions in the prescribed treatment volume. This calculation utilizes the CT data, along with other physical data including measured linear stopping powers versus linear attenuation coefficients, to calculate the average linear stopping powers relative to water for all tissues traversed by pions in reaching the treatment volume. The bolus cross-sections are transferred to styrofoam templates. All the templates are glued together using alignment reference marks to produce a styrofoam bolus model. The model is then encased in a dental impression material, forming a mold into which paraffin is poured to produce the final bolus. Collimators are also designed from computer output.

H. Patient Immobilizaton, Alignment, and Transfer Systems

Immobilization and transfer of patients from pre-treatment staging to the treatment room has evolved in conjunction with changing treatment conditions. The basic approach has remained the same, following the concept of prior immobilization and positioning (PIP). The use of CT scans for precise tumor localization and inhomogeneity compensation led directly to the use of PIP in maintaining the same patient position throughout the CT scanning, localizing radiography, pretreatment set-up, and treatment process.

The use of an orthopedic casting material (Lightcast II) was adopted. The Lightcast shells require additional surrounding support to hold them and the patient in the desired orientation. Immobilization modules, designed by the CRTC team in cooperation with a NASA consulting engineer, have been mounted on the treatment and simulator tabletops. These consist of molded fiberglass trays supported by a framework of heavy stainless steel and aluminum. A tray can be rotated about the long axis and the transverse horizontal axis. Within the tray, the Lightcast shells are supported by a vacuum bag, filled with styrofoam beads, which is evacuated after the patient is in approximate position. The tray is then rotated as necessary to achieve the proper orientation, as indicated by two levels, one in the x-axis and one in the y-axis, on the Lightcast shells. These are attached to the shells during the simulation process when the patient is in the desired treatment position. In addition templates, which are cut to fit the patient contour in both the longitudinal

COPIED FOR
HSPT

1091214

00133339.006

LANL

and transverse directions and fitted with spirit levels, aid in checking the final patient treatment position. Identical couches in the treatment and simulation rooms have a positioning base and a removable tabletop. The positioning base can be used to translate the patient up or down within the horizontal plane.

Using cross-hair lasers in the set-up area (corresponding with identical lasers in the treatment room), the patient can be positioned within the treatment module on a treatment tabletop supported by a transport dolly. Reference tattoos on the patient and alignment marks on the case, bolus, and collimator, help to ensure accuracy of the alignment. The patient is then transported to the treatment room. Upon completion of the previous patient's treatment, the tabletop itself (supporting the patient in his module) is transferred to the treatment table base and aligned under the lasers for treatment. Positioning patients outside the treatment room permits optimization of pion beam utilization, in addition to improving the accuracy of daily dose deposition. About three minutes are required in the treatment room to achieve the final adjustment prior to treatment delivery. An electronic coding scheme has been implemented to permit computer verification that the correct collimator is in place prior to treatment.

I. Computerized Treatment Planning

Work is proceeding on the three-dimensional model in PIPLAN that carries out the actual calculations of the dose deposited in the patient, using their CT-scan data. Techniques have been developed for creating smooth input data that represent the beam configurations used in patient treatments. A new neutron model is being developed that will better account for the neutron dose in the plateau region of the beam. Extensive comparisons with experimental measurements, both in air and water, are being made.

Physics models were added and upgraded which significantly improved the accuracy of the dose calculations. The interactive version of PIPLAN was essentially completed on the Biomed computer system. A variety of changes were included to accommodate the latest clinical setup and treatment requirements.

In the area of CT data, the number of scanners that can be decoded was increased to five, refined experimental data were incorporated into the decoding process, a study was completed to determine required resolution for treatment planning, and specifications relating to treatment planning were incorporated into the CT scanner purchase contract.

The two-dimensional dose calculation programs were upgraded to provide faster input and batch-mode, post-processing to increase throughput with less operator time. Independent calculations of dose distributions in water phantoms were incorporated into these programs, reducing the amount of dosimetry required. Documentation in all areas progressed with increased emphasis.

COPIED FOR
HSPT

1091215

00133339.007

LANL

III. BIOLOGY

A. In Vitro Studies

Two systems have been used to quantitate the effectiveness of pions relative to that of x-rays: single cells (survival and mutagenesis) and multicellular tumor spheroids.

1. Single Cell Survival

Fractional survival of single CHO cells following exposure to a variety of peak pion beams, differing in peak volume, dose rate, and, presumably, LET spectra, has been evaluated. These curves have been compared to those for cells exposed to high intensity (61 rads/minute) small peak volume (8 cm^3) pions or to x-rays (Figure 1). The sole detectable difference between pions and x-rays in multiple experiments has been a reduced shoulder width in the former relative to the latter. Similar observations have been made by Dr. Gloria Li at the Stanford pion facility and by Dr. Christine Lucke-Hukle at the Swiss Institute for Nuclear Research (SIN).

Peak pion beams with volumes of ~800 cm^3 have also been investigated, with the same results (Figure 2). The system is not sufficiently precise to compare the extent of the shoulder shift in the small and large peak volume beams, but it should be noted that a difference could not be detected in the effectiveness between the proximal and distal portions of the expanded pion peak in these studies. This does not mean that total effect is constant across the peak, because total dose drops from 100 to 75 percent from the proximal to the distal peak, but rather that "effectiveness per rad" could not be shown to differ significantly.

A variety of phenomena could account for the reduction in the shoulder of the cell survival curve without a concommittant alteration in slope, with the most likely being a pion-induced interference with sublethal injury repair. If this were the case, one would expect less short-term Elkind-type repair when the pion doses were delivered as two equal doses separated by a matter of hours compared to the same total dose given as a single exposure. Figure 3 is a plot of the survival ratio (survival following two equal doses/ survival following same total dose as a single exposure) for high intensity peak pions or x-rays as a function of the time in hours between the two exposures. Elkind-type repair is apparent in the groups given paired doses of x-rays and in those given paired doses of pions, but it is far less pronounced in the latter than in the former, as would be expected if the reduced shoulder on peak pion cell survival curves (Figures 1 and 2) reflected a reduced ability to repair sublethal injury.

Although sublethal injury repair has not been studied in all of the cell lines maintained in our laboratory, the straight single-cell survival studies have been extended to include a variety of other cell lines. The results of these studies are summarized in Figure 4. As with CHO cells, the only detectable difference between pion and x-ray single-cell survival curves for these other lines is a reduction in the shoulder of the cell survival curve without a detectable alteration in slope.

COPIED FOR
HSPT

1091216

00133339.008

LANL

Kligerman, H.H.
[redacted] 5-P01-CA-14052-06

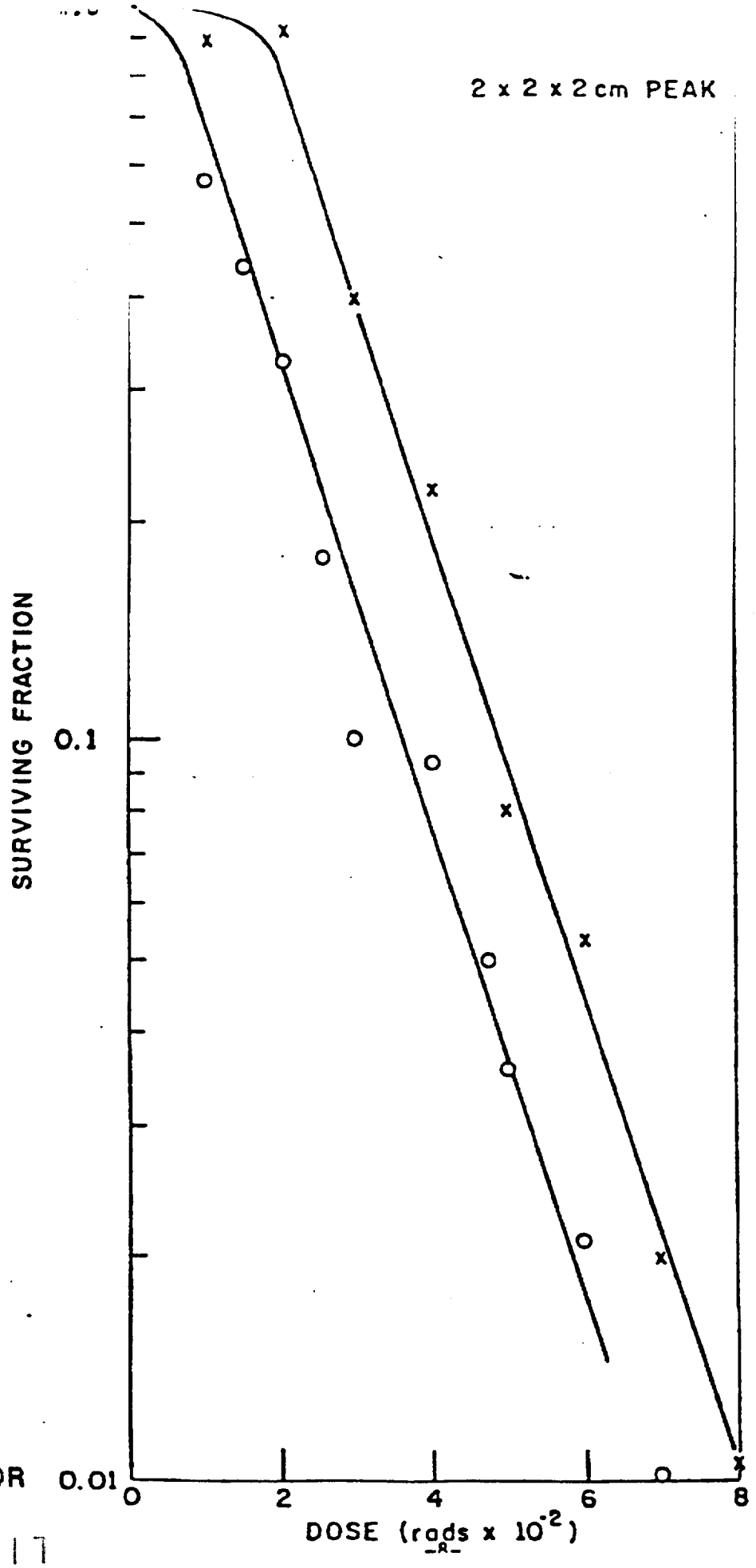

Figure 1. Survival of CHO cells exposed to single doses of x-rays (x) and peak pions (o), 2 x 2 x 2 cm beam

COPIED FOR
HSPT
1091217

00133339.009

LANL

COPIED FOR
HSPT

Kligerman, M.M.
[redacted]
5-P01-CA-14052-06

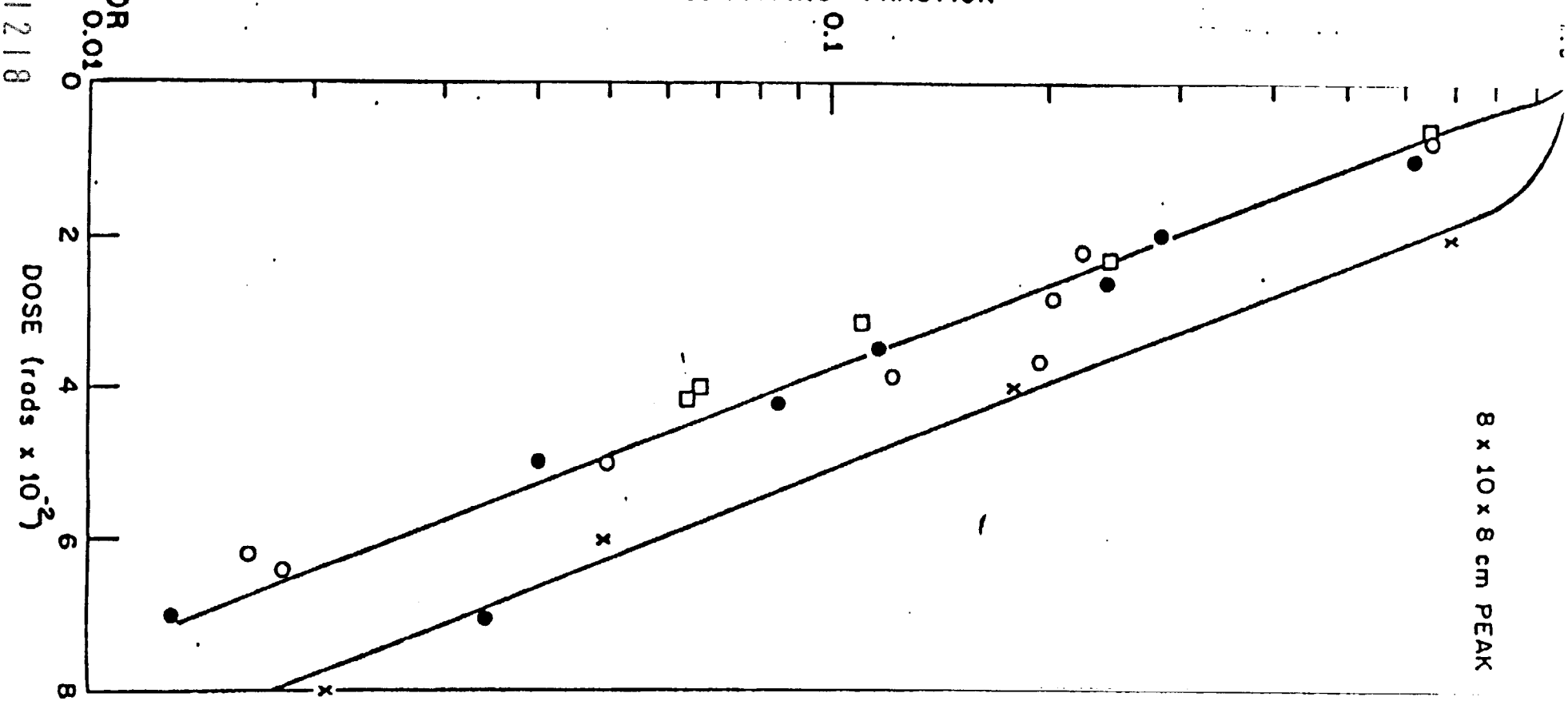

Figure 2. Survival of CHO cells exposed to single doses of x-rays (x) and peak pions (● = 1 cm, o = 4 cm, ■ = 7 cm), 8 x 10 x 8 cm beam

1091218
00133339.010
LANL

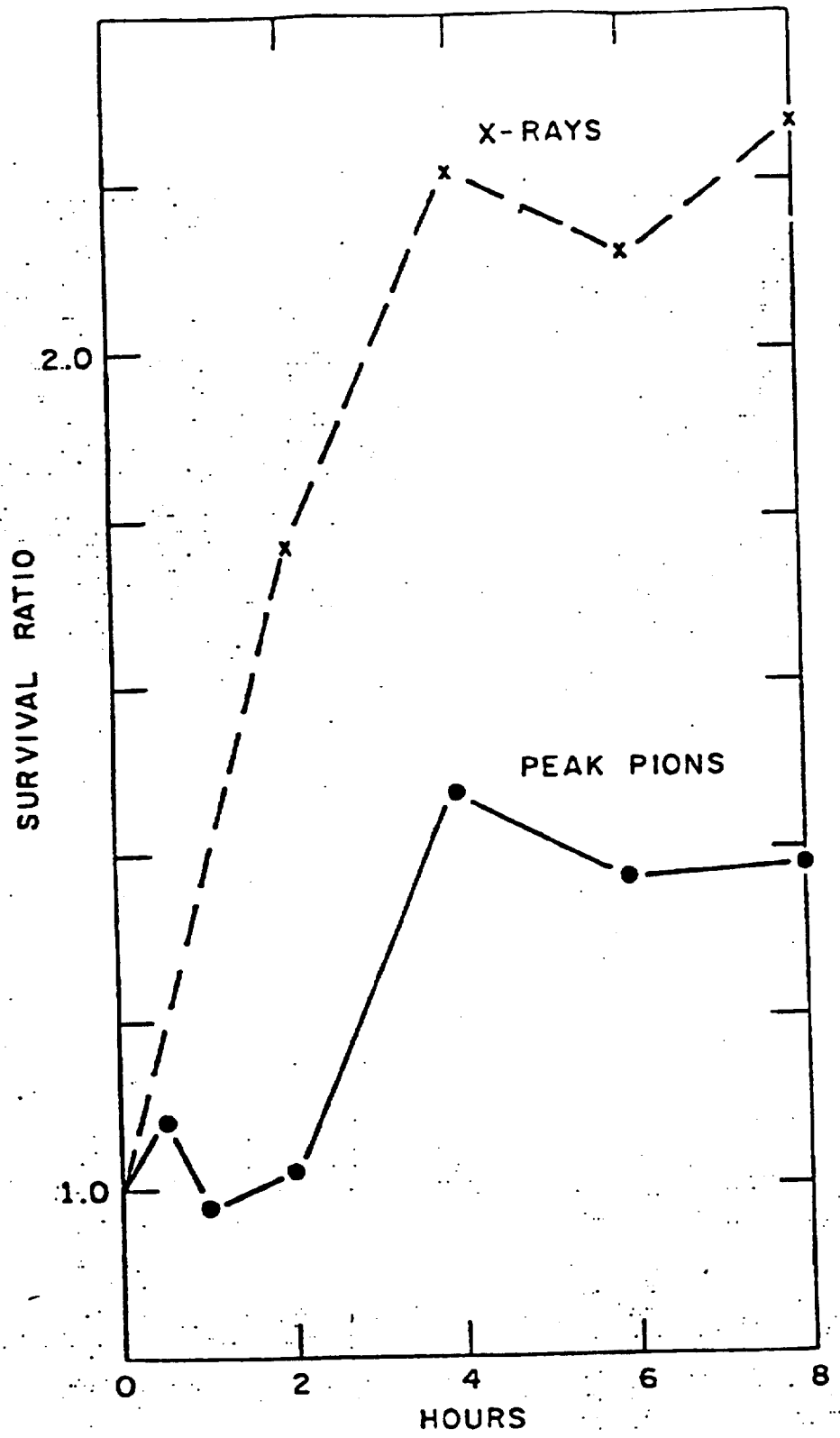

COPIED FOR
HSPT

Figure 3. Survival ratio of CHO cells: survival following two equal doses ÷ survival following same total dose as single exposure

1091219
00133339.011
LANL

Figure 4. Survival of other than CHO cells exposed to single doses of x-rays and pions

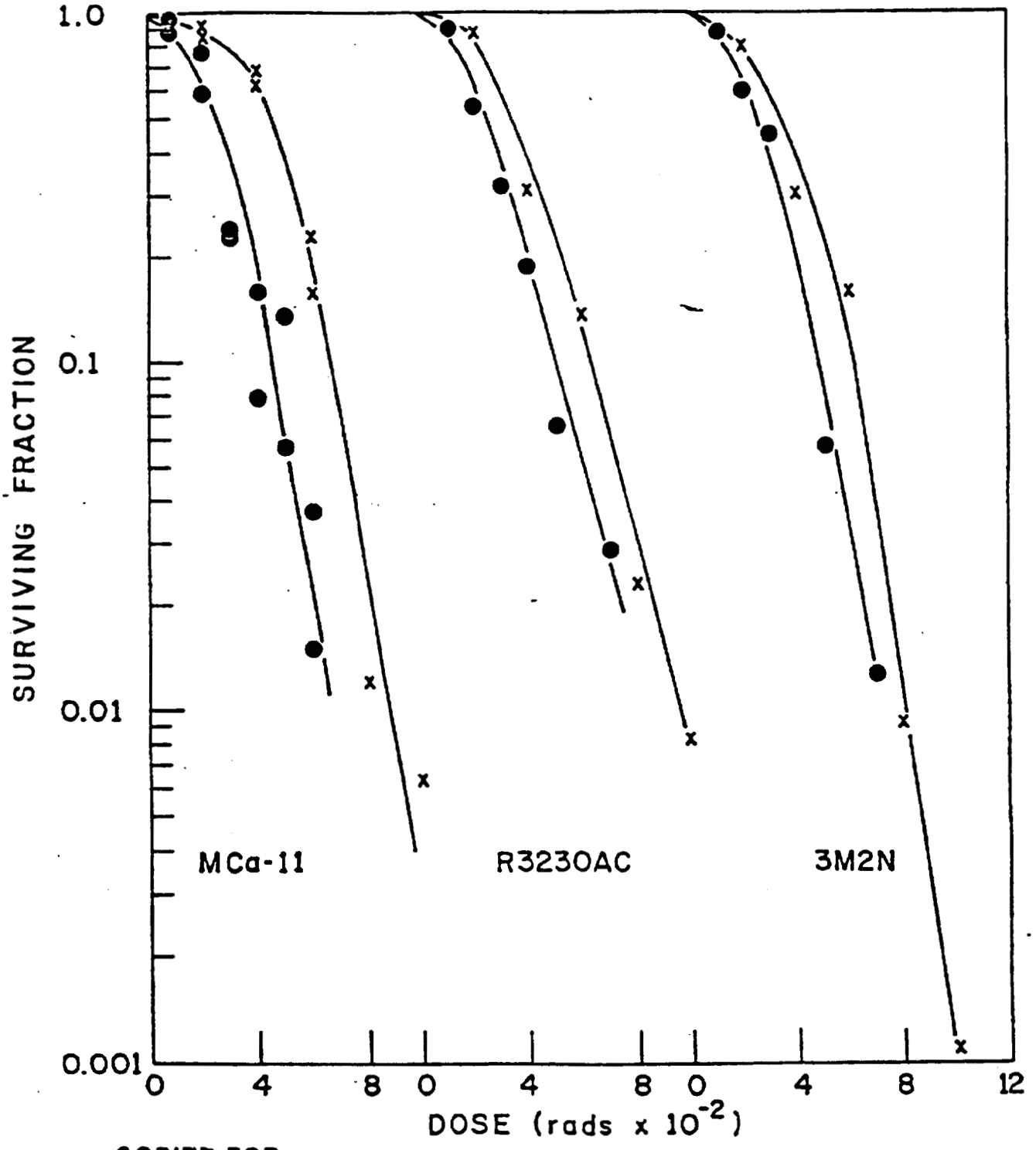

COPIED FOR
HSPT

1091220

00133339.012

LANI

With present technology it is not possible to identify the LET spectra pertinent to small volumes approximating the size of biological targets, so the physical basis for these observations remains unclear. Empirically, however, the question of peak pion interactions with true low-LET radiations, i.e., x-rays, can be addressed. If a component of the peak pion dose can inhibit the repair of sublethal injury induced by the low-LET portions of the peak dose, it should also be able to inhibit repair of sublethal injury induced by x-rays. To test this, CHO cells were exposed to doses of x-rays (Figure 5a) or peak pions (Figure 5b) that would reduce survival to ~10%. Four hours later, graded doses of x-rays or peak pions were administered. As shown in Figure 5, the only combination that allowed the return of the shoulder was x-rays followed by x-rays. No shoulder reappeared in x-rays following pions, pions following x-rays, or pions following pions because (1) sublethal injury repair was inhibited, and/or (2) the shoulder on the pion curve was reduced.

These observations suggest that pions are producing the same type of phenomenology as has been observed in the past by Ngo and Elkind for neutrons and by Ngo, more recently, for heavy ions. In brief, administration of high-LET radiation prior to x-rays can alter the tolerance of the cells to the accumulation of low-LET sublethal injury. While this type of observation is unexpected, it has been reported a sufficient number of times by different groups to warrant further study, although the underlying mechanisms remain to be established.

As shown in Figure 6, administration of x-rays immediately after relatively low peak pion doses produces a large reduction in the size of the x-ray curve shoulder, but the mechanism underlying this reduction remains unclear. Whatever the ultimate mechanism, these observations could explain how one obtains similar cell survival curves in spite of the fact that peak pion beam quality is altered, either by use of different peak volumes or by placing the cells at different positions within the peak.

2. Mutagenesis Studies

Because the CHO cell used in our studies can readily be assayed for the induction of somatic mutations at the HGPRTase locus, cells from single-cell survival studies were saved for determination of the rate of pion-induced mutation relative to that for x-rays. Three points evolved from these studies which bear on the basic radiobiology of pions: (1) the slope for mutants per 10^6 survivors versus dose is three times steeper for pions than it is for x-rays (Figure 7); (2) the yield of mutants is independent of the peak employed (Figure 8); and (3) peak pions can sensitize CHO cells to the induction of mutations by x-rays (Table 1).

TABLE 1

Effects of Graded Doses of 2-cm Peak Pions on Ability of 50 Rads of X-Rays to Induce Somatic Cell Mutations at HGPRTase Locus

Radiation Dose (rads)		Mutants/10^6 Survivors		
X-ray	Pions	Expected	Observed	Excess
50	50	15.9	27.5	11.6
50	100	20.1	31.2	10.1
50	200	47.7	60.2	12.5

COPIED FOR HSPT
00133339.013
1091221
LANL

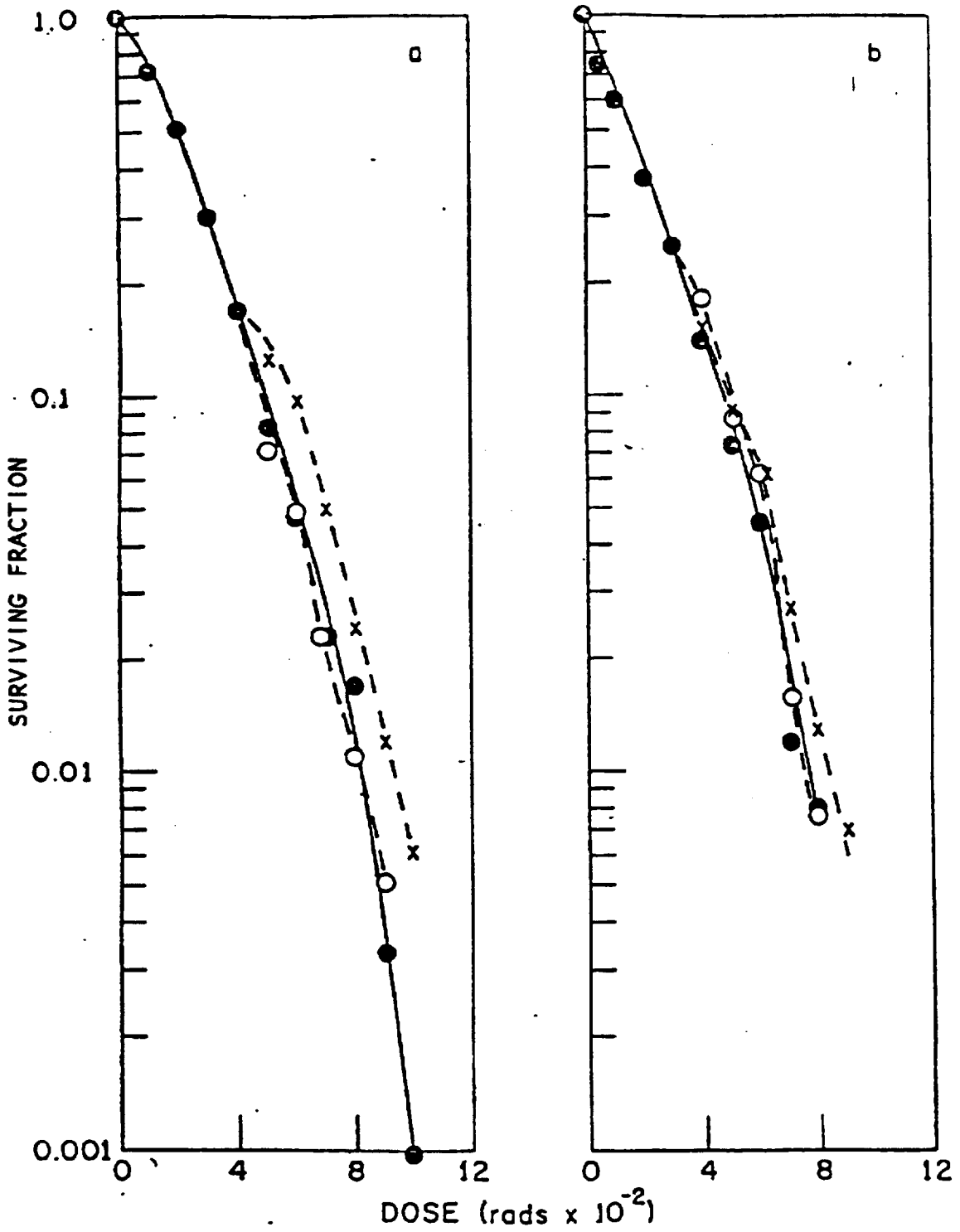

Figure 5a. Survival of CHO cells exposed to x-rays, followed 4 hours later by a second dose of either x-rays (x) or pions (o).

Figure 5b. Survival of CHO cells exposed to pions, followed 4 hours later by a second dose of either x-rays (x) or pions (o).

COPIED FOR
HSPT

LANL

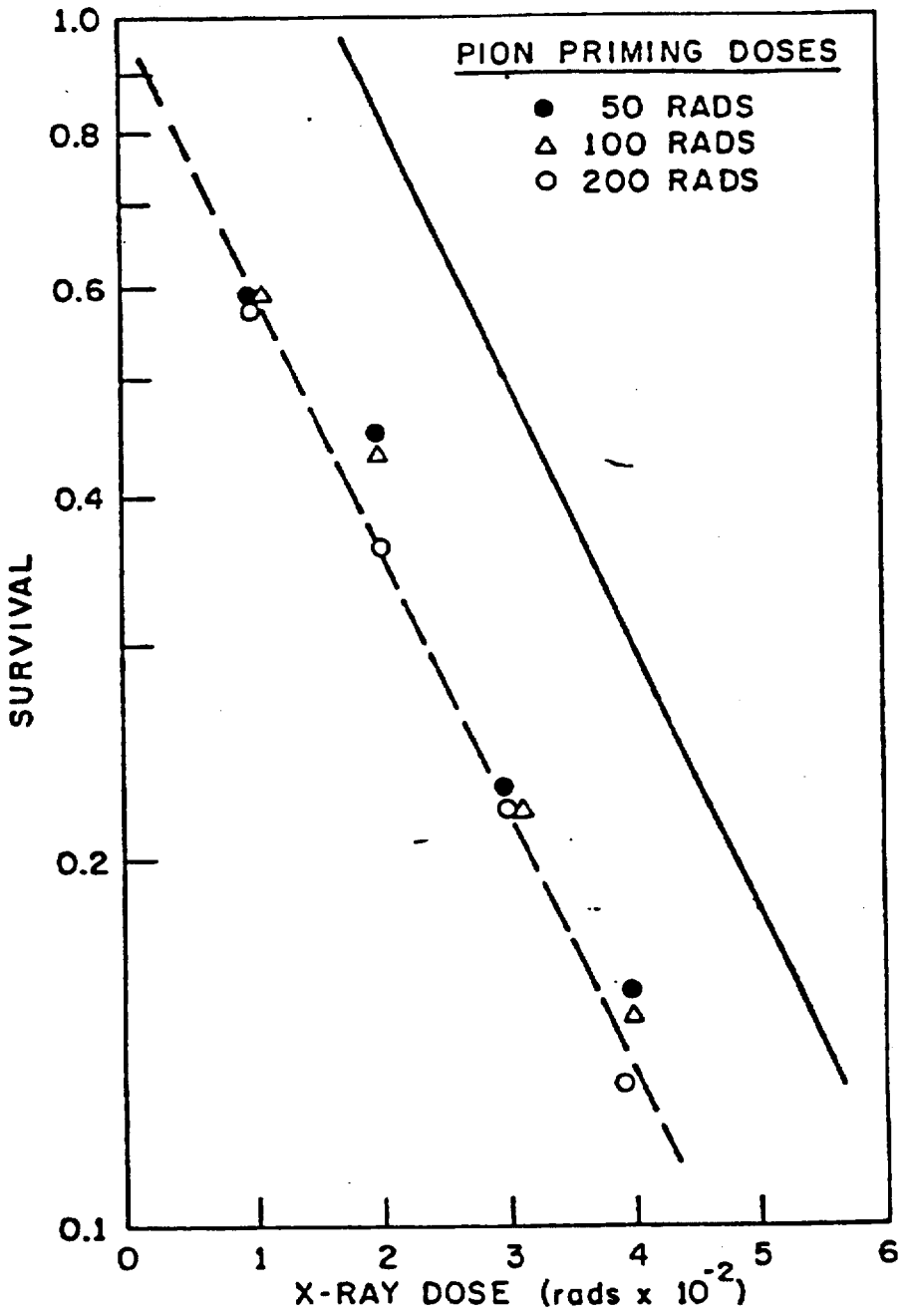

Figure 6. Survival of CHO cells exposed to 50, 100, and 200 rads of pions followed immediately by graded doses of x-rays.

COPIED FOR
HSPT

1091223

00133339.015

LANL

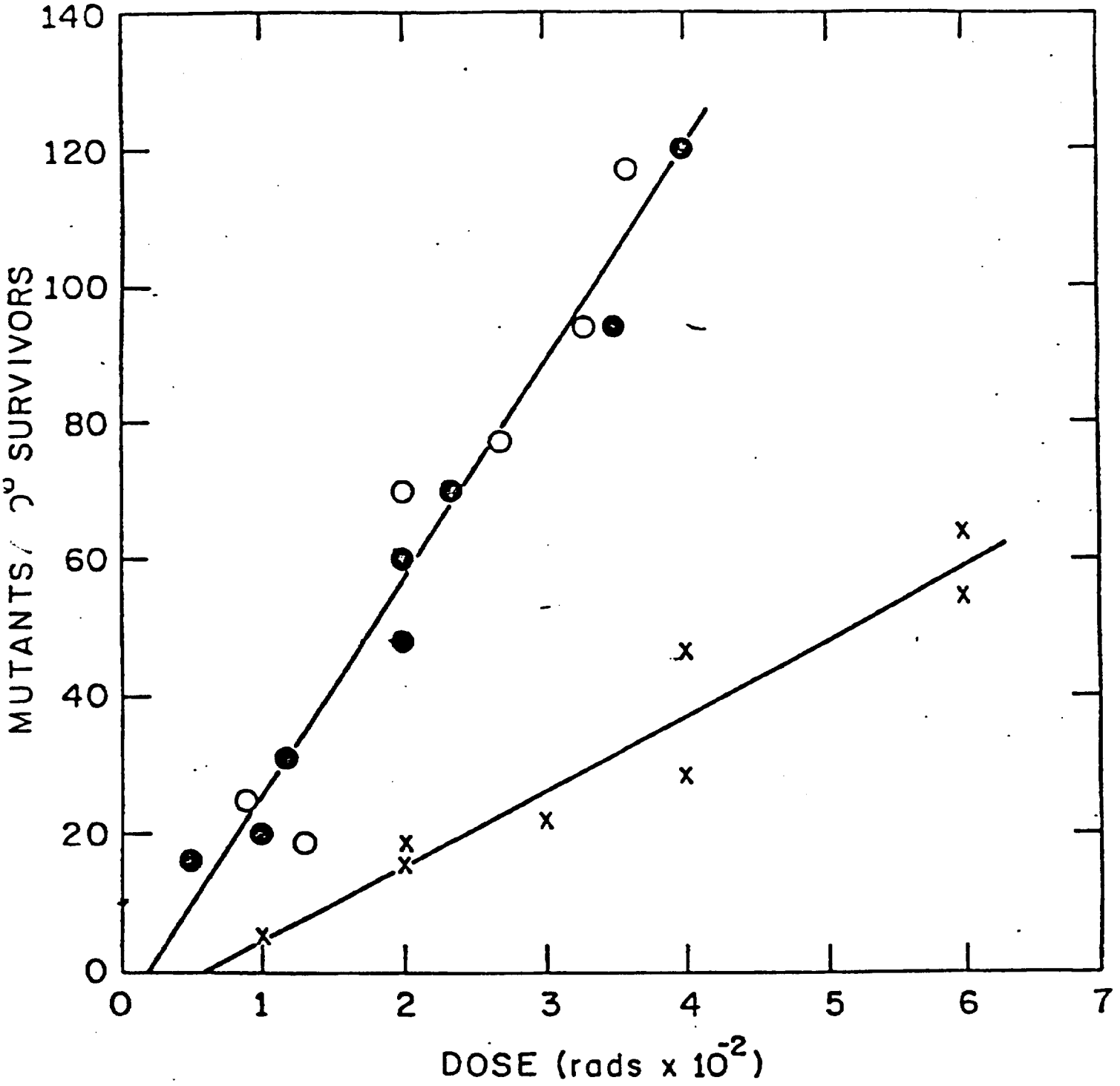

Figure 7. Mutants per million surviving CHO cells, x-rays (x) versus pions (open and closed circles from 2 separate experiments).

COPIED FOR
HSPT

1091224
00133339.016
LANL

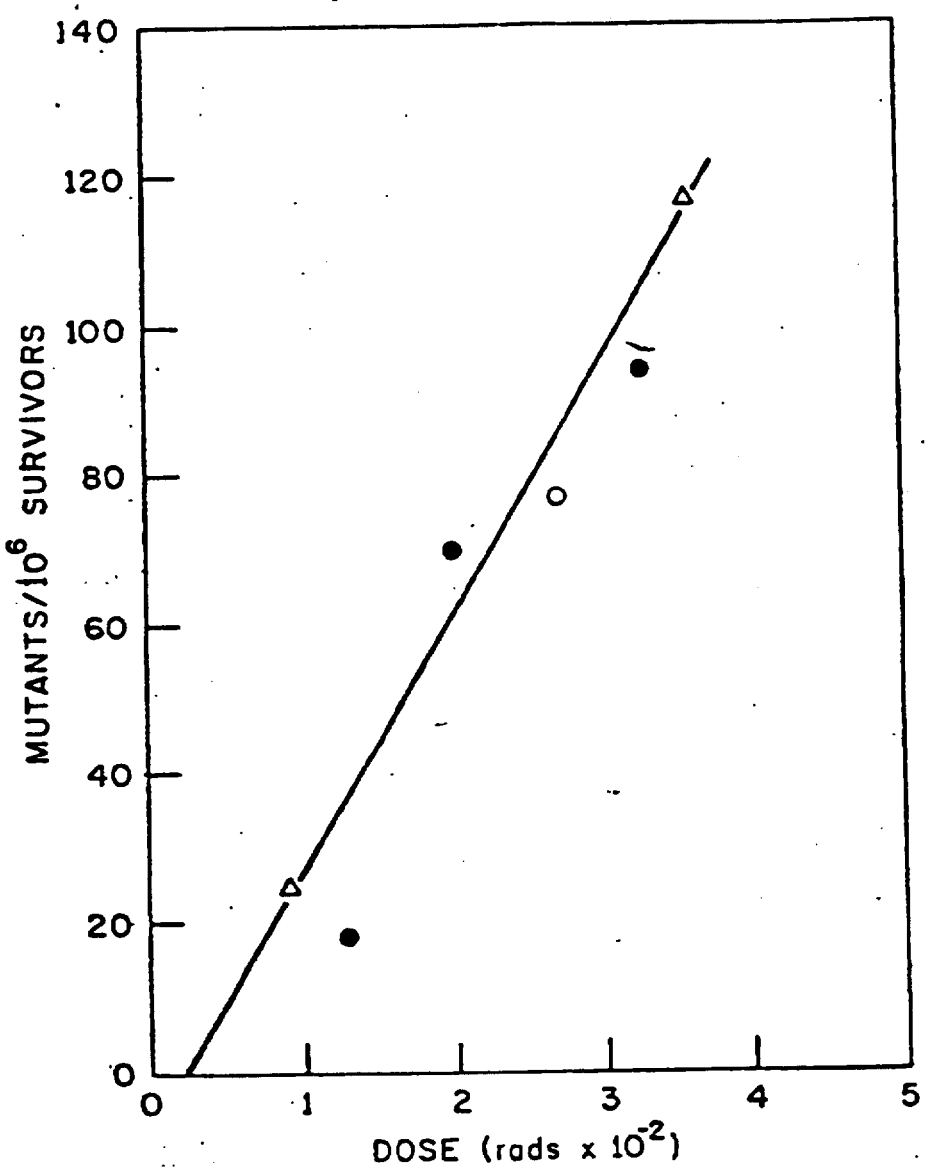

Figure 8. Mutants per million surviving CHO cells, as a function of pion dose. (● = 8 cm^2 peak; ▲ = 125 cm^3 peak; ○ = 800 cm^3 peak).

COPIED FOR
HSPT

1091225

00133339.017

LANL

These studies indicate that pions are three times more effective than x-rays for production of single-hit-type injury (for both radiations log-log slopes of mutants on dose = 1.0), and that in this highly quantitative system one also observes peak volume independence and "sensitization" to x-ray type injury.

3. Multicellular Tumor Spheroid Studies

In contrast to single cells, tumors are heterogenous with subpopulations of cells differing in their oxygenation status, cycle characteristics, and other factors. To develop an understanding of how tumors would respond to pions, within the available beam time constraints, the *in vitro* multicellular tumor spheroid (MTS) system developed in the CRTC laboratories was used. These MTS were exposed to radiation and then sized three times weekly until they grew an additional 200 to 300 μm. Data were expressed as the radiation-induced delay in time to reach a given size, similar to the expression of data for *in vivo* tumor experiments (see below). Figure 9 is a typical set of curves for Line 1 lung carcinoma MTS exposed to peak pions, x-rays, or peak pions followed immediately by x-rays. The sole difference between peak pions only and x-rays only is that the pion curve is shifted to the left; *i.e.*, a smaller threshold dose must be exceeded before one obtains delay being proportional to dose. Analogous to the single-cell survival data, the curves for delay versus dose are parallel once their respective thresholds are exceeded.

In the group given both pions and x-rays, the effect of the pion dose has been corrected for the pion-induced delay; yet the curve remains shifted to the left; *i.e.*, the exposure to 50 rads of pions has "sensitized" the MTS to x-rays delivered immediately thereafter. A clearer presentation of this phenomenon is given in Figure 10. Conditioning doses of 50, 100 or 200 rads of pions totally eradicated the threshold for x-ray growth delay. In contrast, the amount of threshold reduction was directly related to dose size when conditioning doses of x-rays were studied.

The extent of threshold reduction varied with the specific MTS studied, and the results obtained with an MTS line that lacks a threshold, even for x-rays, is instructive. Figure 11 shows that in this no-threshold system, pions and x-rays are quantitatively identical because the only difference between pions and x-rays is expressed at the level of the threshold.

These MTS have also been used to quantitate the effects of multiple fractions of pions relative to the same for x-rays. Figure 12 is a plot of the growth delay induced by 1 and 10 daily fractions of pions and x-rays in the MCa-11 MTS system. Under both single-dose and multiple-dose studies the pion and x-ray curves are parallel, but the data for the two types of fractionation are not parallel to each other. Table 2 summarizes the estimated RBE values, which offer an approximate comparison with the *in vivo* normal tissue data presented below.

COPIED FOR
HSPT

1091226

00133339.018

LANL

Figure 9. Radiation-induced delay in growth of multicellular tumor spheroids (MTS) for peak pions (●), x-rays (x), and peak pions followed immediately by x-rays (o).

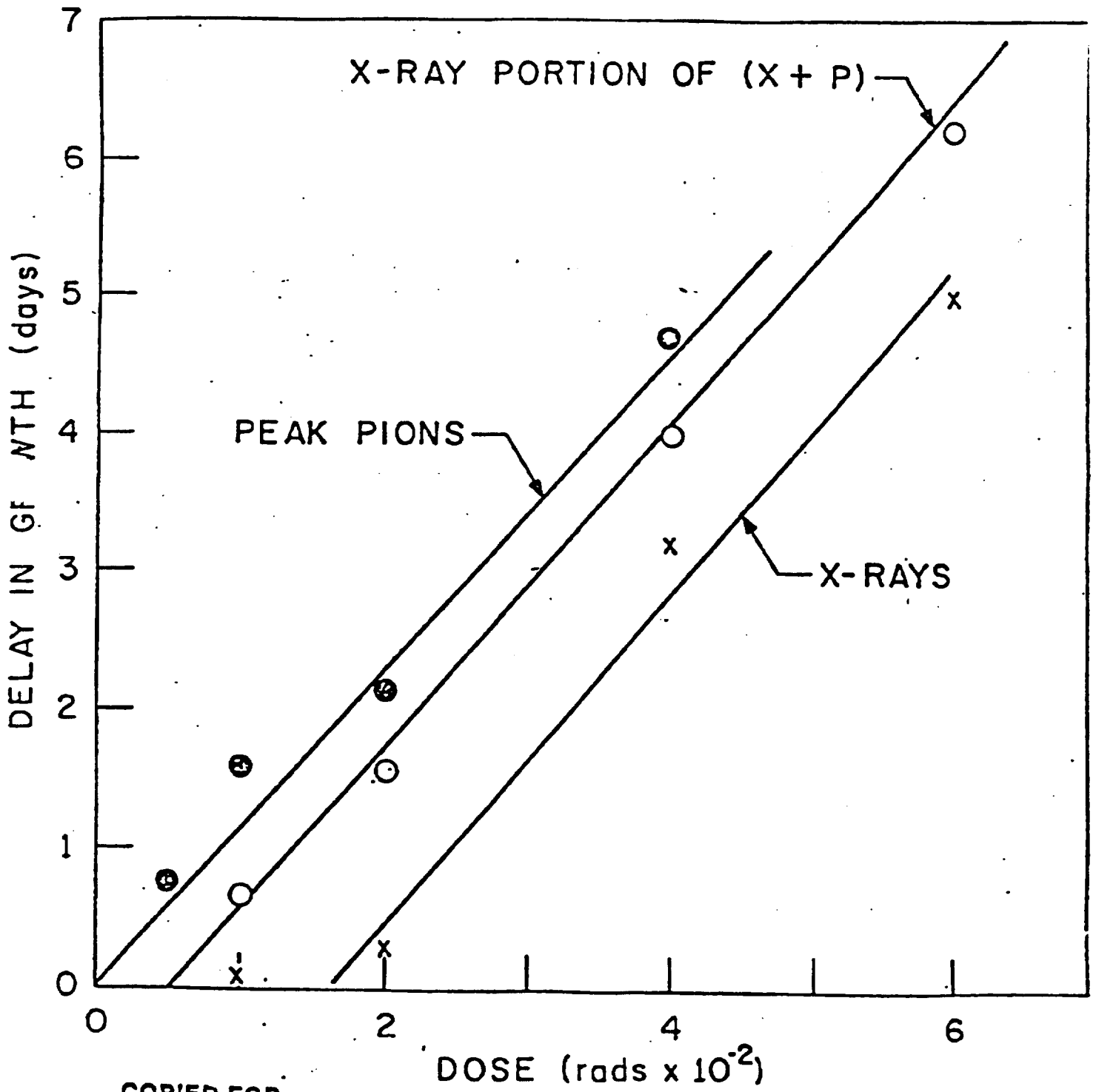

COPIED FOR HSPT

00133339.019
1091227
LANL

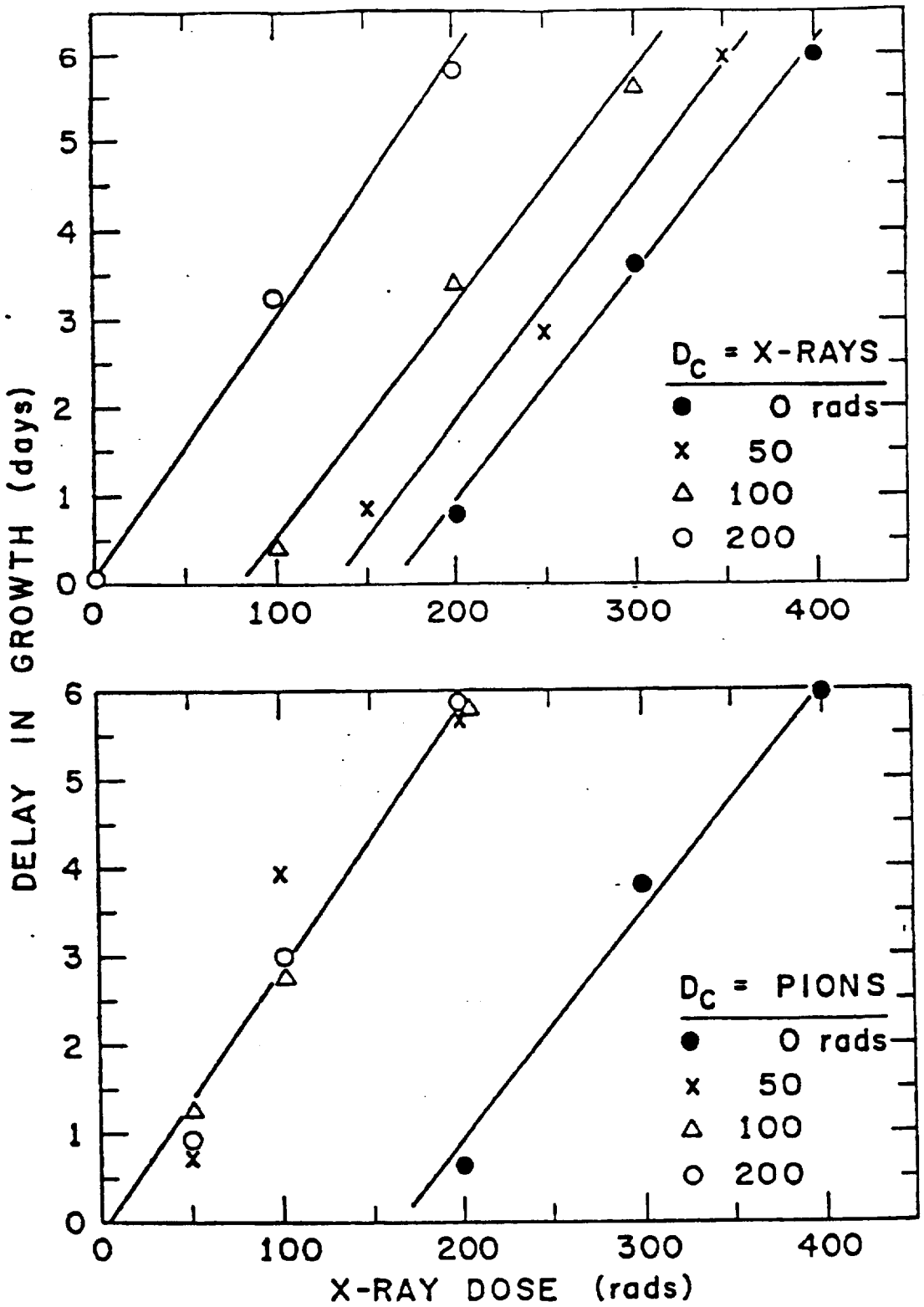

Kligerman, M.H.
[redacted]
5-P01-CA-14052-06

Figure 10. Effects of 50, 100, and 200 rad conditioning doses (Dc) of peak pions and X-rays on the sensitivity of MCa-11 MTS to graded doses of X-rays delivered immediately afterward.

COPIED FOR
HSPT

1091228

00133339.020

LANL

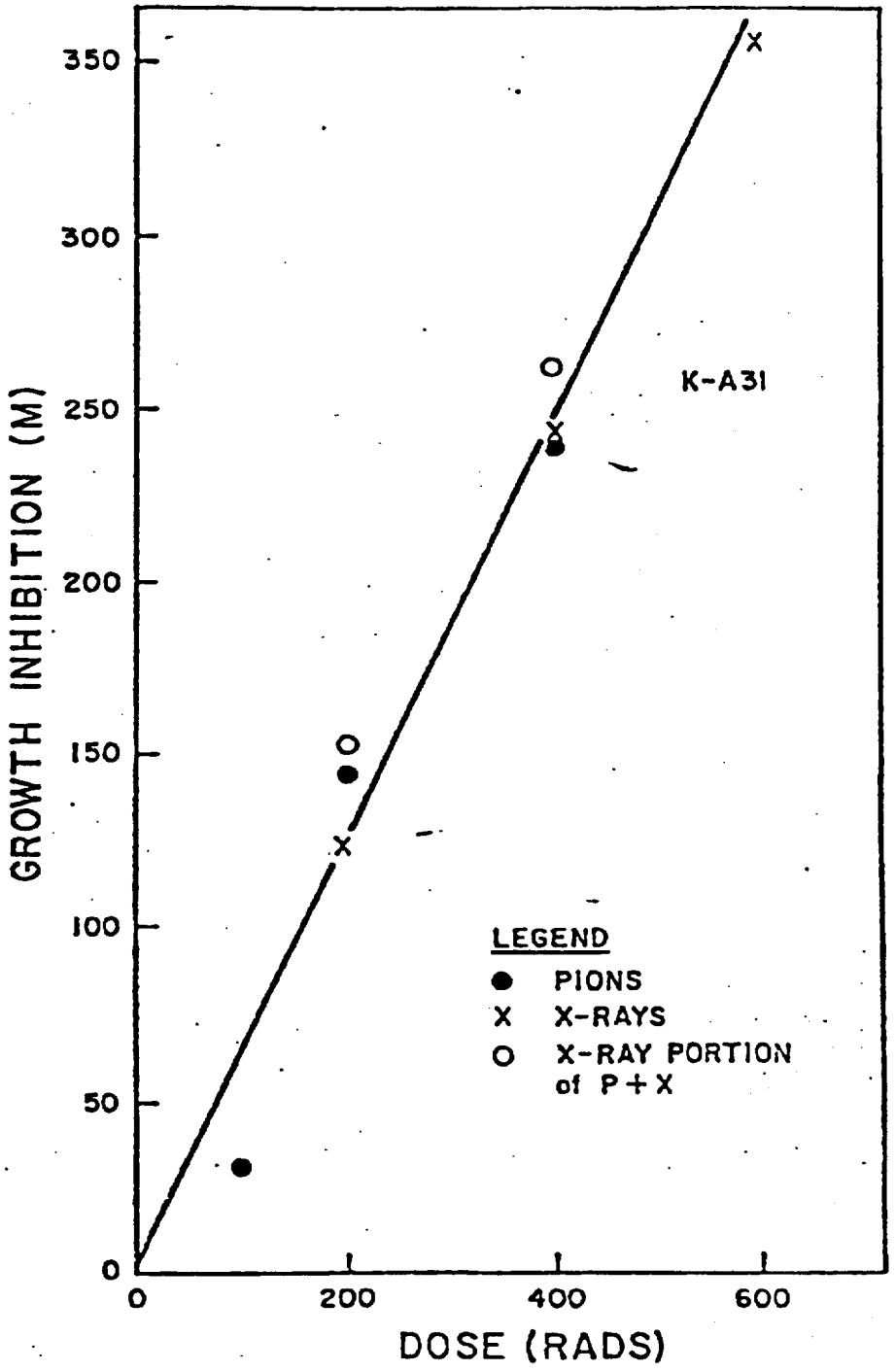

Figure 11. Growth inhibition versus dose (pions and/or x-rays) for K-A31 MTS.

COPIED FOR HSPT

1091229
00133339.021
LANL

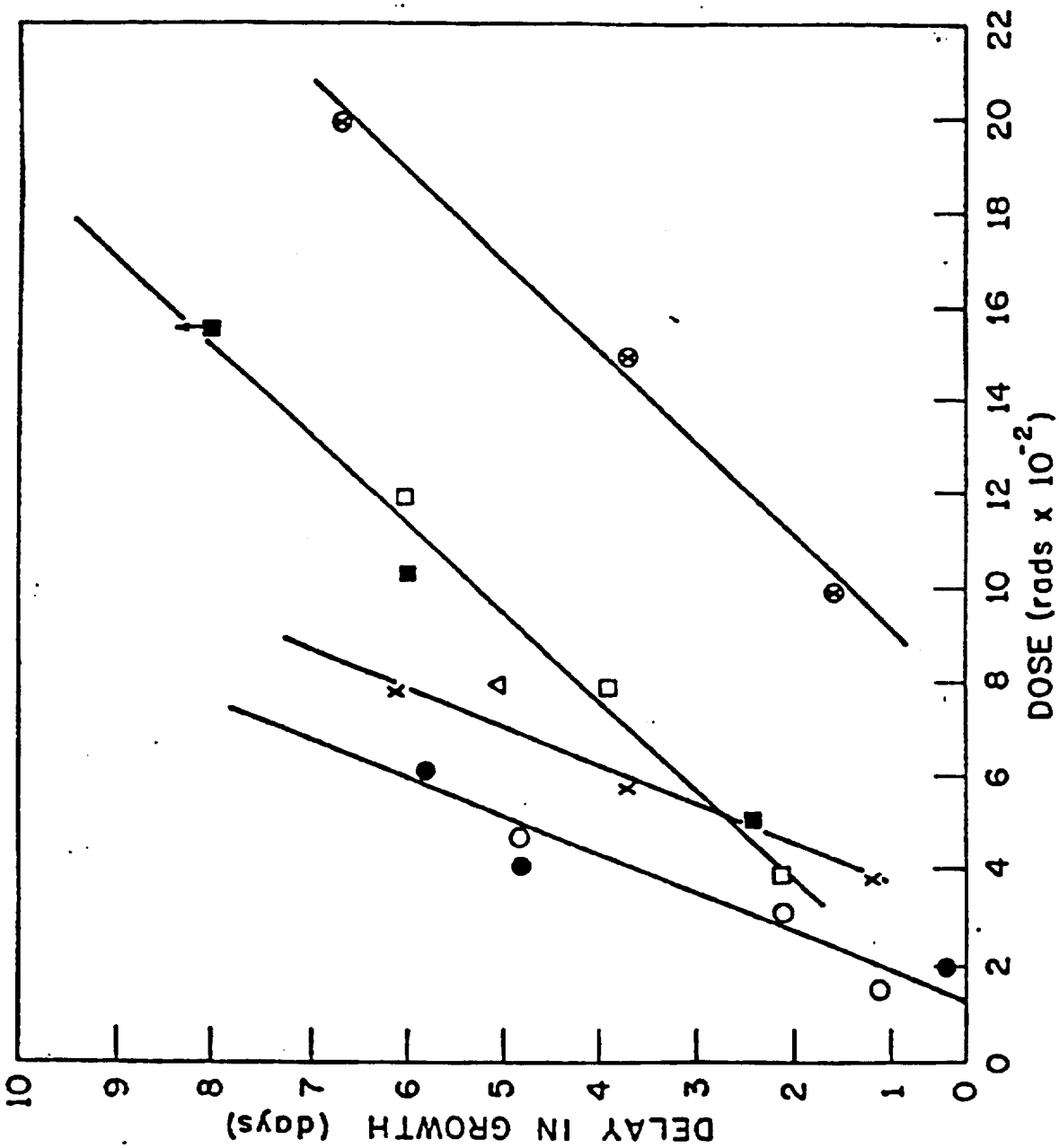

Figure 12. Radiation-induced delay in growth, single versus multiple doses. (X = single dose x-ray; ⊗ = 10 daily x-ray doses; ○, ● = proximal and distal peak, single pion doses; □, ■ = proximal and distal peak, 10 pion fractions

COPIED FOR
HSPT

1091230
00133339.022
LANI

TABLE 2
Relative Biological Effectiveness (RBE) for Pions, Following Single-Fraction and Multiple-Fraction Exposures of Multicellular Tumor Spheroids

Growth Delay (Days)	One Fraction (X-ray/Pion = RBE)		Ten Fractions (X-ray/Pion = RBE)	
	MCa-11 Experiment #1			
2	480/360	1.33	1140/540	2.11
4	630/510	1.24	1520/820	1.85
	MCa-11 Experiment #2			
2	464/273	1.70	1108/402	2.76
4	630/436	1.44	1500/781	1.92
	Line-1 Lung			
2	610/500	1.22	1390/860	1.62
4	1030/905	1.14	2350/1585	1.48

B. In Vivo Studies

1. Tumor Studies

Mice bearing the MCa-11 mammary tumor were exposed to graded total doses of high-intensity peak pions or X-rays either as single fractions or as three daily fractions. Figure 13 is a plot of the delay in time to grow 4 mm beyond the original size as a function of total dose for each of the groups. The data are not sufficient to determine whether the single dose curves are parallel, but it is readily apparent that pions are 1.2 - 1.4 times more effective than x-rays in the single dose studies and that the delay induced by three daily doses of pions is almost as large as that induced by single pion doses, while that for x-rays shows far greater tumor recovery from fractionation. More detailed studies on this system are in progress.

2. Kidney Studies

These studies have been described by Jordan et al. (Arch. Pathol., in press). In brief, the remaining kidney of unilaterally nephrectomized mice was exposed to peak pions or x-rays one month after nephrectomy. Six months after exposure they were sacrificed for histologic examination and semi-quantitative grading of their kidney injury. Figure 14 is a plot of the RBE of pions as a function of the number of daily fractions in this system. Studies involving up to 15 daily fractions are in progress.

3. Spinal Cord Studies

An initial study on pion vs. x-ray induced spinal cord paralysis in the rat was conducted at a dose rate of 6 rads per minute. Figure 15, which summarizes the one-year paralysis data from this experiment, suggests an RBE of ~1.5. These studies have been repeated using 1 or 15 fractions and all are summarized in Table 3, through 5 months post-exposure. Clearly pions are

COPIED FOR
HSPT 1091231
00133339.023
LANL

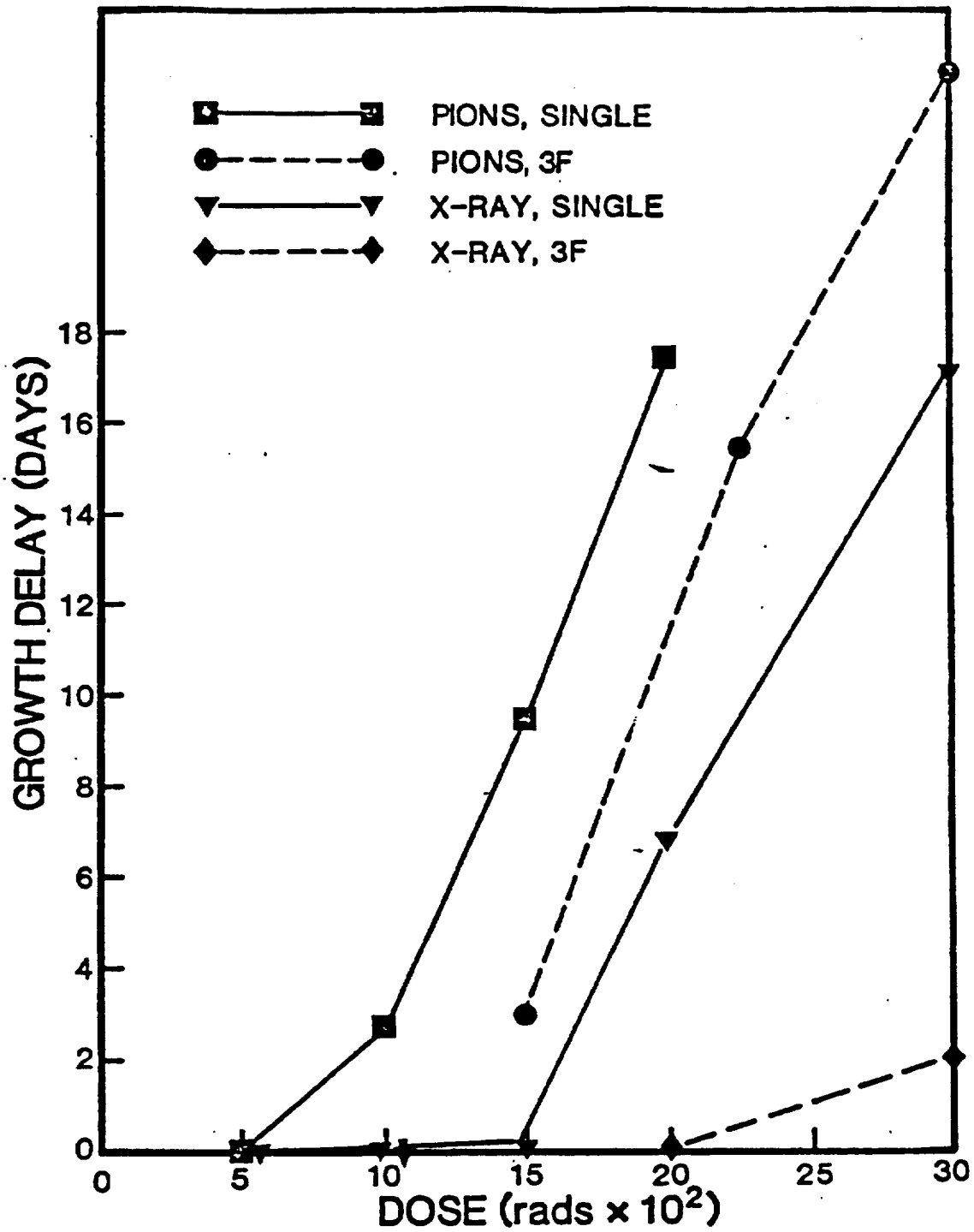

Figure 13. Radiation-induced delay in growth as a function of total dose.

COPIED FOR
HSPT

1091232
00133339.024
LANL

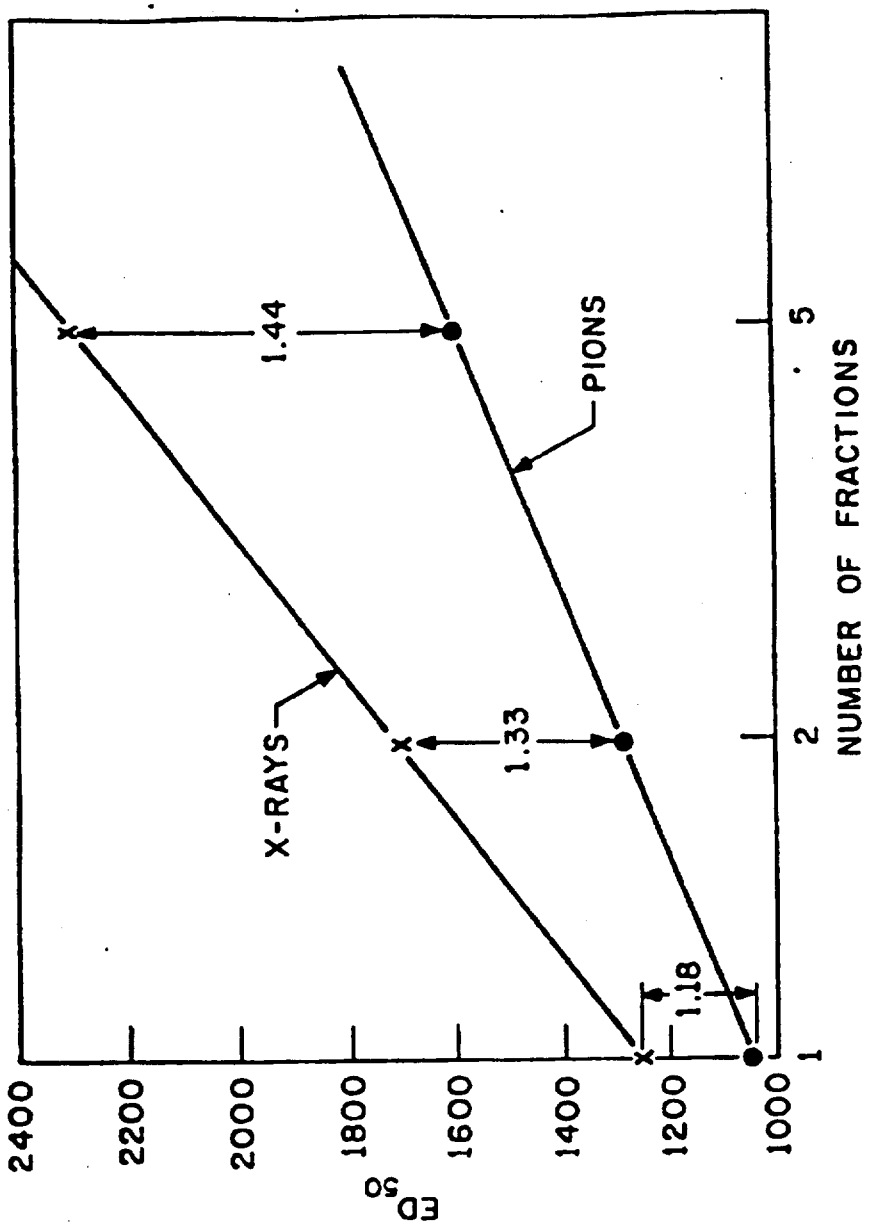

Figure 14. Dose required to produce grade 3 kidney injury in 50% of the irradiated group as a function of the number of daily fractions of x-rays (X) or peak pions (●) delivered. RBE values are given within a fractionation pattern on the vertical arrows.

COPIED FOR
HSPT

1091233

00133339.025

LANL

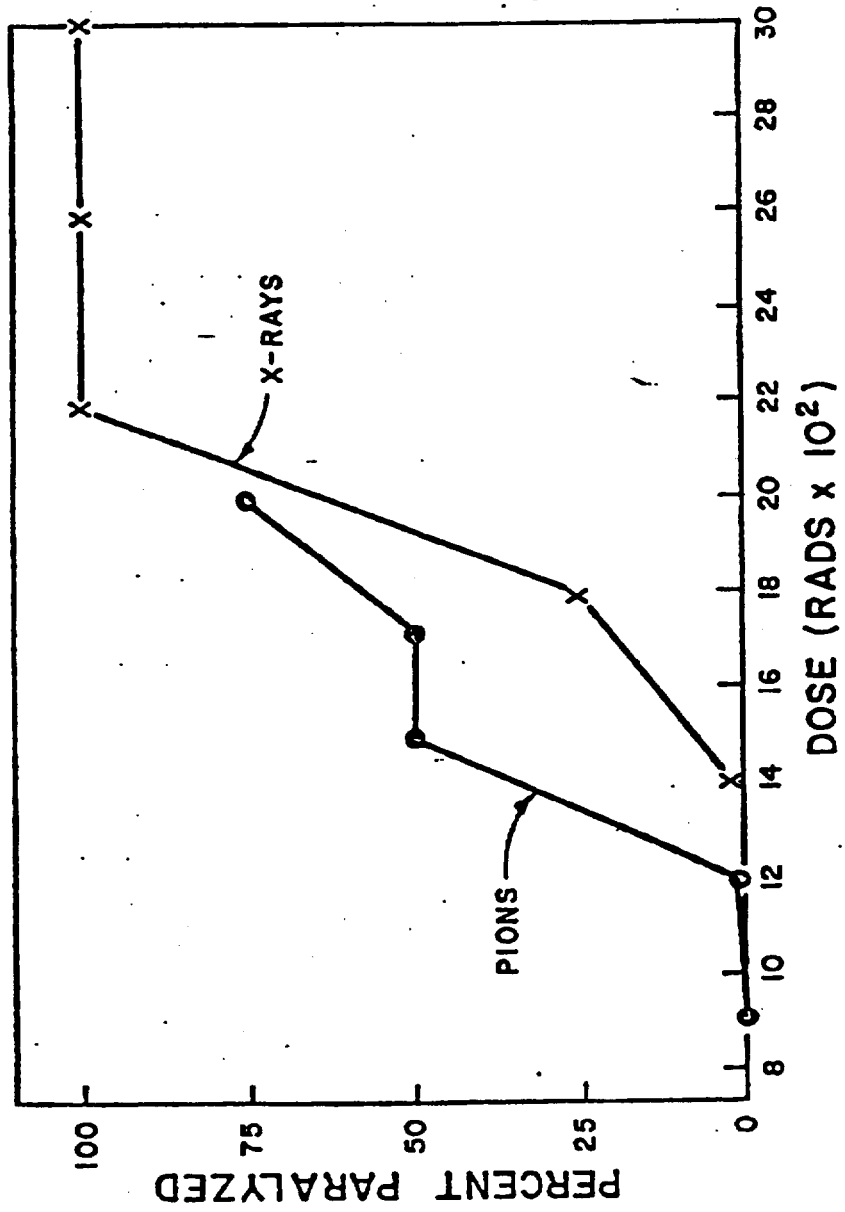

Figure 15. Cumulative spinal cord paralysis in rats through 1 year following exposure to peak pions (6 rads/min) or x-rays.

COPIED FOR
HSPT
1091234

00133339.026
LANL

far more effective than x-rays in inducing spinal cord paralysis than are x-rays, especially under conditions of repeated fractionation. Calculation of RBE at this time would not be warranted, since paralysis is appearing rapidly in all groups. Further, the pion doses listed are nominal as the apparently high pion RBE might reflect a "bone/soft tissue" interface problem.

TABLE 3

Frequency of Radiation-Induced Paralysis in Rats Through Five Months after Exposure to 1 or 15 Fractions of X-Rays or Peak Pions

	Single Dose to Spinal Cord		Historical
Rads	Pions	X-Rays	X-rays
1800	6/6	0/6	0/6
2000	6/6	0/6	1/6
2200	6/6	0/6	4/6
2400	6/6	2/6	6/6
2600	6/6	6/6	6/6
	15 fractions to spinal cord		
2000	0/6		
2400	0/6	0/6	
2800	2/6		
3000		0/6	
3200	6/6		
3600	6/6	0/6	
4000	6/6		
4200		0/6	
4800		0/6	
5400		0/6	
6000		0/6	

4. Colon Studies

The development of this system for studying the late fibrotic and vascular injury in the colon of rats is complete and has been described by Black et al. (Cancer, in press). Studies involving up to three daily fractions have been completed and are summarized in Figure 16. Preliminary 15-fraction studies have been initiated.

5. Lung Studies

Three studies involving radiation-induced lung death and/or collagen deposition have been initiated, but none of the mice has successfully survived the treatment. The mice uniformly develop chronic pneumonia and die. No further lung studies are contemplated.

COPIED FOR
HSPT

1091235

00133339.027

LANL

Figure 16. Dose of pions (●) or X-rays (x) required to produce minimally toxic late radiation injury in the rat colon as a function of the number of daily treatments. RBE's are given on the vertical arrows.

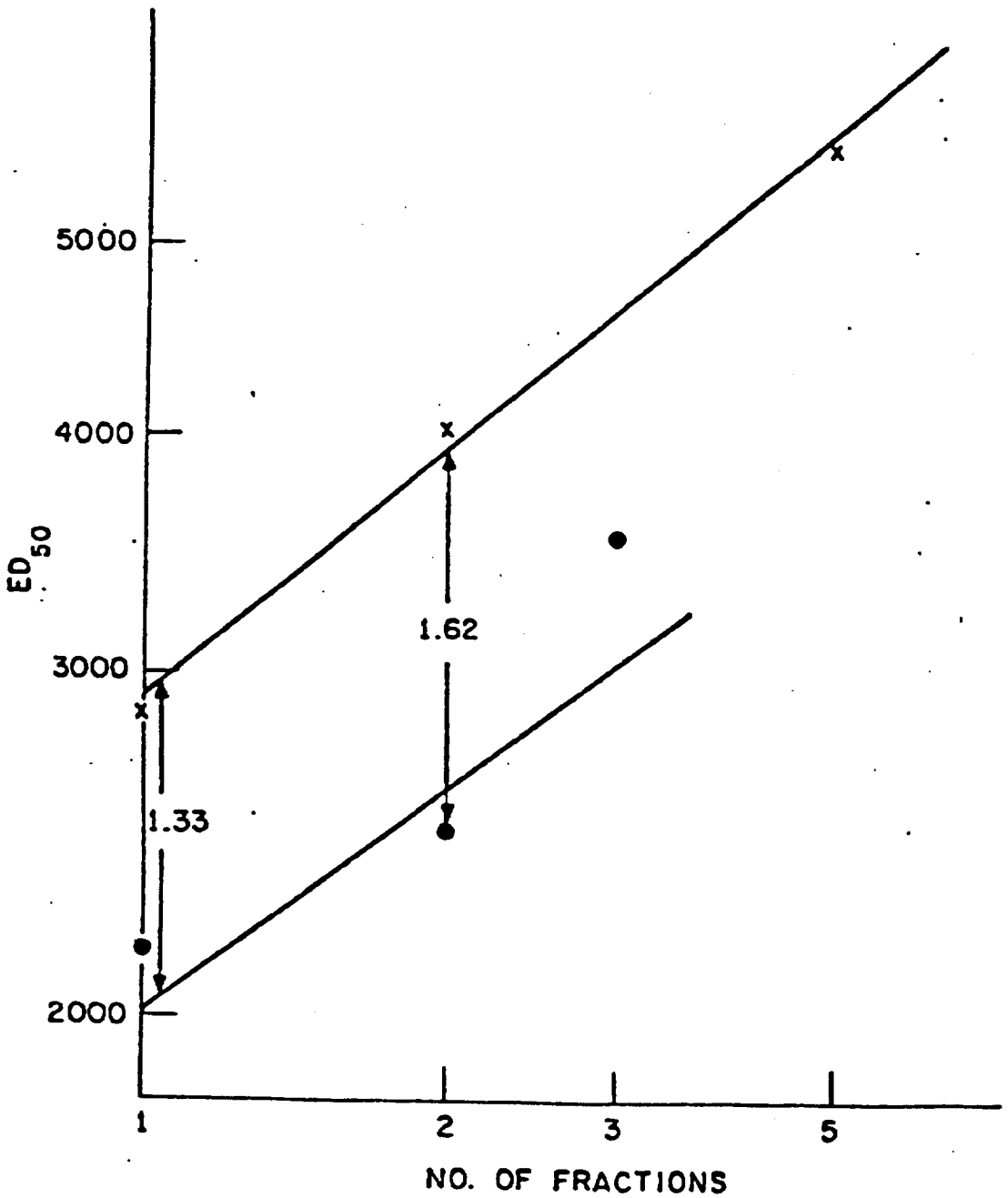

COPIED FOR
HSPT

1091236
00133339.028
LANL

6. Heart Studies

Limited heart studies in rabbits are in progress.

7. Skin Studies

Table 4 summarizes the 1- and 5-fraction skin studies performed thus far. Scoring of skin reactions has been performed on all the fractionation studies, and a better understanding of skin reactions to fractionated pions is expected, once the doses received by the skin in various internal organ studies are reconstructed.

TABLE 4

Total Doses of 2-cm Peak Pions or 300 kVp X-Rays Required to Induce Moist Desquamation in BALB/C Mice.

	X-rays	Pions	RBE
Single Fraction	2392 ± 108	1623 ± 89	1.47
5 Daily Fractions	3760 ± 148	2284 ± 211	1.65

IV. FUTURE PLANS

The work described above is continuing under Grant No. 2-P01-CA-16127-06. Plans and progress after 30 April 1979 will be routinely reported in the continuation applications for that grant.

COPIED FOR
HSPT

1091237
00133339.029
LANL

logged

THE UNIVERSITY OF NEW MEXICO

Copied From Los Alamos
National Laboratory Archives

DATE: December 12, 1979

TO: DISTRIBUTION

FROM: Stephany Wilson, Administrator, CRTC at Los Alamos SW

SUBJECT: Terminal Progress Report, CA-14052-06

T050

Attached, for your review and file, is a copy of the final terminal progress report for the above-referenced grant. Please let me know if you have any questions about it.

SW:mm

Attachment

DISTRIBUTION:
Dr. Bradbury, MP-3
Dr. Smith, CRTC
Dr. Bush, CRTC
~~R. Warner, MP-DO~~
R. Peterson, FMO, LASL

FILE BARCODE
00133336

COPIED FOR
HSPT

1091238

REPOSITORY LANL/ARC
COLLECTION MP-DO
BOX No. A-91-011
FOLDER 180-5
00133336.001

COPIED FOR
HSPT

DEC 12 1979

CANCER RESEARCH AND TREATMENT CENTER
THE UNIVERSITY OF NEW MEXICO ■ ALBUQUERQUE, NEW MEXICO 87131
900 CAMINO DE SALUD NE ■ TELEPHONE 505: 277-2151
MORTON M. KLIGERMAN, M.D., Director

December 7, 1979

Floyd A. Frazier
Division of Cancer Research
Resources and Centers
National Cancer Institute
National Institutes of Health
Bethesda, Maryland 20205

REF: Grant No. 5-P01-CA-14052-06

Dear Mr. Frazier:

Attached are the original and three copies of a terminal progress report for the above-referenced grant. We apologize to you for the lateness of this report. We did not realize until we received your letter of October 29, 1979, that a terminal progress report was required, as the work has been transferred to another grant (2-P01-CA-16127-06) and is being reported under continuation applications for that grant.

In any event, we have compiled a progress report for you and trust it will be satisfactory. If you need anything further from us, please do not hesitate to call.

Sincerely,

M. Kligerman

Morton M. Kligerman, M.D.

Warren Baur

Warren D. Baur
Fiscal Director, UNM Medical Center

SW:vdj

Attachment

FILE BARCODE
00133337

00133337.001

1091239

LANL